J. Membrane Biol. 11, 75–97 (1973)

A Barrier Model for Current Flow in Lipid Bilayer Membranes

James E. Hall, C. A. Mead, and Gabor Szabo

Department of Electrical Engineering, California Institute of Technology, Pasadena, California 91109 and Department of Physiology, University of California School of Medicine, Los Angeles, California 90024

Received 7 April 1972

Summary. The *shape* of the energy barrier inside thin, insulating membranes can be an important factor in determining the detailed behavior of transmembrane ionic flows. In particular, a model is developed in which the shape of the barrier is expected to have direct influence on such experimentally important membrane properties as: (a) the shape of the current-voltage relation; (b) the dependence of zero current conductivity on asymmetric concentrations; (c) the dependence of the rectification ratio on the concentration ratio.

Current-voltage curves were measured for a wide range of symmetrical and asymmetrical concentrations in black lipid (phosphatidyl ethanolamine) films in the presence of nonactin and potassium. A single barrier shape was found to describe accurately the experimental results in terms of the model.

The electrical behavior of black lipid (bilayer) membranes formed in aqueous solutions of hydrophylic ions is similar to that of a thin insulating film (Mueller, Rudin, Tien & Wescott, 1962; Hanai, Haydon & Taylor, 1964). Such behavior arises largely from the great cost in energy required to move a charge into the insulating region. In the case of black lipid films, this energy barrier is likely to result from the low dielectric constant of the hydrocarbonlike membrane interior.

Lipophilic ions or small amounts of ionophorous neutral macrocyclic molecules (Pressman, 1968) that render alkali cations lipid soluble by complexing with them (Pioda, Wachter, Dohner & Simon, 1967; Shemyakin *et al.*, 1969) are observed to increase bilayer conductivity by many orders of magnitude (Mueller & Rudin, 1967) as a result of a selective lowering of the energy barrier to transmembrane ionic movement. In the presence of neutral macrocyclic molecules, the identity of the current-carrying species is known and the behavior of the membrane conductance is well documented

(Andreoli, Tieffenberg & Tosteson, 1967; Lev & Buzhinsky, 1967; Tosteson, 1968; Szabo, Eisenman & Ciani, 1969).

Current-voltage (I–V) curves observed both in the presence (Buzhinsky, 1968; Szabo *et al.*, 1969) and absence of neutral ionophores are generally nonlinear and of two types: either the current increases faster than the voltage or the current increases more slowly than the voltage and reaches some saturating value. Careful examinations of possible mechanisms responsible for nonlinear I–V curves in bilayer membranes were made by Walz, Bamberg and Läuger, 1969; Neumcke and Läuger, 1969*a*, *b*; and more recently by Läuger and Stark, 1970; Stark and Benz, 1971; Stark, Ketterer, Benz and Läuger, 1971.

In this paper we shall analyze I–V curves where the current increases more steeply than the voltage, in terms of a barrier model which is found to be able to account for the experimentally observed I–V behavior of bilayers in the presence of nonactin and K^+ over a wide range of concentrations.

The Barrier Model

We address ourselves to the relationship between the rate of transmembrane ion translocation and the detailed energetic environment an ion encounters within the membrane. We believe that the I–V curves, in cases where the important rate-limiting step is the flow of ions or charged complexes across the membrane, can be understood in terms of two assumptions: first, that the flow is proportional to the gradient of the electrochemical potential $\psi(x)$[1] of the charged species, and second, the electrochemical potential is given by the sum of the electrical potential $\phi(x)$, the concentration potential $\ln(c(x)/c(0))$, and an invariant barrier function $\omega(x)$, which represents the energy cost of moving an ion from place to place inside the membrane. The existence of such a barrier function can be easily inferred from the observations, first, that the hydrocarbon interior of the membrane is of much lower dielectric constant than the aqueous solutions bathing the film and, second, that a considerable amount of energy is required to move an ion from a region of high dielectric constant to a region of low dielectric constant. For simplicity, we also make the assumptions that the electric field is constant in the membrane[2], diffusion coefficients are constant

1 All potentials will be expressed in units of kT/*e* and all energies in units of kT.

2 This is a good assumption if the charge in the membrane is small and the approximation $d^2\psi/dx^2 \simeq 0$ holds for Poisson's equation; *see* Walz *et al.*, 1969 for a discussion of the conditions when this is so.

within the membrane, activities and concentrations are equal and that all of the voltage drop occurs across the membrane. We will present experimental evidence for the validity of this model in the case of the nonactin-potassium complex.

The electrochemical potential $\psi(x)$ is given by

$$\psi(x)=\omega(x)+\ln(c(x)/c(0))+\phi(x) \tag{1}$$

where c is the concentration of univalent cationic species and $\phi(x)$ is the electrical potential. The current density J will then be given by

$$J=-eD\left(\frac{dc}{dx}+c\frac{d\phi}{dx}+c\frac{d\omega}{dx}\right) \tag{2}$$

where e is the charge per unit concentration (e.g., per mole or per molecule) and D is the diffusion constant of the permeant species. The concentration will thus be an explicit function of position which adjusts itself in such a way that J is fixed for a given voltage across the membrane. We use the constant field approximation to give $\phi(x)=-ux/d$, where u is voltage across the membrane. The solution to Eq. (2) is then

$$J=\frac{2eD}{d}\frac{c_1 e^{u/2}-c_2 e^{-u/2}}{\int_{-1}^{1} e^{\left[\frac{u\xi}{2}+\omega(\xi)\right]}d\xi}, \tag{3}$$

where c_1 is the concentration on the left boundary, c_2 the concentration on the right boundary, and d is the membrane thickness. For simplicity we express the integral in terms of ξ, the dimensionless distance coordinate given by $\xi=2x/d$.

The above derivation follows directly that of Neumcke and Läuger, 1969*b*. They, however, *calculated* $\omega(\xi)$ from an image charge model, while we will reexamine this approach from another point of view and treat the barrier $\omega(\xi)$ as a *measurable function*. The validity of the model will be checked by how well a single barrier shape can explain results obtained over a wide range of experimental conditions.

The Influence of Barrier Shape on Current-Voltage Characteristics

Before proceeding to the interpretation of experimental results, it will be useful to consider several specific barrier shapes and the nature of the results to be expected in each case. This will help to form an intuitive idea of the conditions of applicability of the barrier model.

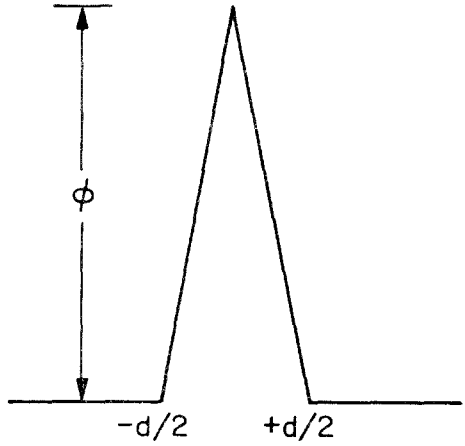

Fig. 1. A triangular barrier of height ϕ and thickness d. The current-voltage relation for this barrier is given by Eqs. (5) and (6)

First, let us consider the simple triangular barrier shown in Fig. 1 described by:

$$\omega(x)=\phi\left(1-\frac{2|x|}{d}\right), \quad \frac{d}{2}\leqq x\leqq\frac{d}{2}; \qquad \omega(\xi)=\phi(1-|\xi|), \quad -1\leqq\xi\leqq 1. \tag{4}$$

Eq. (3) for the membrane current becomes for this triangular barrier:

$$J=\frac{2eD}{d}\frac{e^{-\phi}(c_1 e^{u/2}-c_2 e^{-u/2})}{\frac{(e^{(\frac{u}{2}-\phi)}-1)}{\left(\frac{u}{2}-\phi\right)}+\frac{(1-e^{-(\frac{u}{2}+\phi)})}{\left(\frac{u}{2}+\phi\right)}}. \tag{5}$$

We note that if the applied voltage is much less than the height of the barrier ($e^{-\phi}\ll 1$), the result simplifies to

$$J=\frac{eD\phi}{d}e^{-\phi}(c_1 e^{u/2}-c_2 e^{-u/2}). \tag{6}$$

If the concentrations are equal on both sides of the membrane ($c_1=c_2$) the current-voltage curve is then of the form

$$J=\frac{2eDc}{d}\phi e^{-\phi}\sinh(\tfrac{1}{2}u). \tag{7}$$

The important part of this result, namely that the current varies with the hyperbolic sine of the voltage multiplied by *one-half* (and not some other number), is often applied in essentially *a priori* fashion. (*See*, for

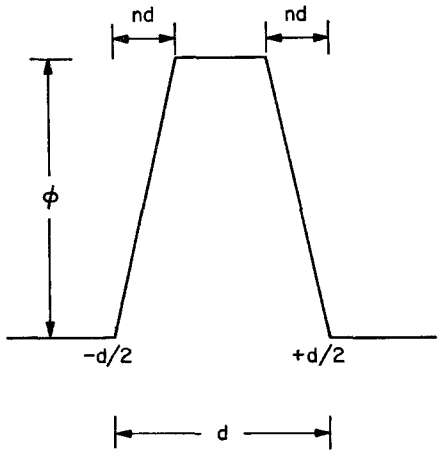

Fig. 2. A trapezoidal barrier with thickness d at the base and thickness $(1-2n)d$ at the top. This barrier is shown in Fig. $3a-d$ for various voltages and concentrations

example, Läuger & Stark, 1970). Several simply derived consequences of the form of barrier giving rise to I–V relations of Eq. (7), are not generally recognized. In particular, the influence of barrier shape on I–V curves expected in asymmetrical solutions has not been considered.

We use the form of the I–V curve given in Eq. (6) for simplicity in making the point. If the current is to be zero, the voltage must be

$$u_0 = \ln \frac{c_2}{c_1}. \tag{8}$$

We now inspect the form of the current-voltage curve when the voltage is measured with respect to the resting potential u_0.

$$J(\Delta u) = \frac{eD}{d} \phi e^{-\phi} \sqrt{c_1 c_2} \sinh(\Delta u/2), \qquad \Delta u = u - u_0. \tag{9}$$

Consequently, the I–V curve will be symmetric about the resting potential *even for asymmetric concentrations* and the zero current conductivity will be proportional to $\sqrt{c_1 c_2}$. Clearly, the rectification ratio $|J(+\Delta u)/J(-\Delta u)| = 1$ even with asymmetric solutions.

It should be carefully noted at the point that these results are a direct consequence of the specific shape of the barrier, and hold only for a barrier which has a sharp maximum in the center of the membrane. To show this explicitly, let us consider the trapezoidal barrier of Fig. 2. We start with the case of symmetric solutions. If a positive voltage is now applied, the barrier

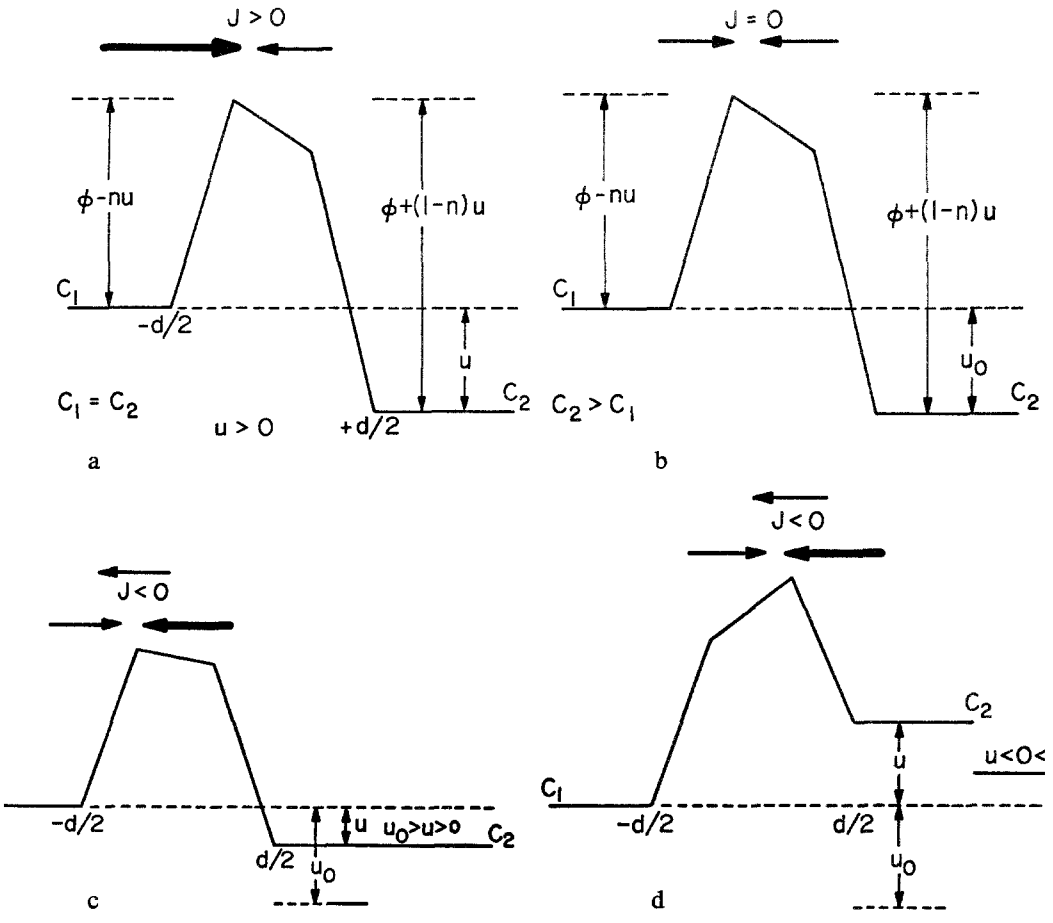

Fig. 3. (*a*) A trapezoidal barrier with equal concentrations on both sides and a positive voltage u applied. The net current can be thought of as the sum of a current from right to left and one from left to right, as indicated by arrows. The barrier to flow of ions from left to right is $\phi - nu$ while that to flow from right to left is $\phi + (1-n)u$. (*b*) A trapezoidal barrier with asymmetric concentration ($c_2 > c_1$). The membrane potential u_0 is given by $u_0 = \ln(c_2/c_1)$. As in (*a*), the current may be decomposed into left-to-right and right-to-left components, but now since u equals u_0 these currents are equal but opposite as shown schematically by arrows of equal size. (*c*) A trapezoidal barrier with asymmetric concentrations ($c_2 > c_1$) and u lying between 0 and u_0. Here the important part of the current is from right to left (large arrow) and the voltage dependence is determined by how the barrier for ions in the c_2 reservoir changes. Since the barrier is given by $\phi + (1-n)u$ the current will have an exponential slope of $(1-n)$. (*d*) A trapezoidal barrier with asymmetric concentrations ($c_2 > c_1$) and a negative applied voltage. Here the important current is from right to left but the highest point of the barrier is now the right-hand corner. Consequently, the current will be determined by the barrier of height $\phi - nu$ to ions moving from right to left

will appear as in Fig. 3*a*. Since the differential equation [Eq. (2)] describing the current flow is linear, we can think of the total membrane current as being composed of a current flowing from left to right and a current flowing from right to left. We see that in Fig. 3*a* the highest part of the barrier is closer to the left side of the membrane than to the right. If we assume this highest part to be the most important, the current flow from left to right will be proportional to the number of ions that have sufficient energy to surmount this barrier. This number will in turn be, according to the Boltzmann relation, proportional to the exponential of minus the maximum barrier height. From the geometry of the barrier and the constant-field approximation, the barrier for current flow from left to right will be $\phi - nu$, where ϕ is the maximum barrier height with no voltage applied. Similarly, the barrier for current flow from right to left will be $\phi + (1-n)u$ (*see* Fig. 3*a*). If the sign of the voltage were reversed ($u<0$), the right-hand corner of the barrier would become important. Thus, we can write

$$J = \begin{cases} Ge^{-\phi}(ce^{nu} - ce^{-(1-n)u}), & u>0 \\ Ge^{-\phi}(ce^{(1-n)u}ce^{-nu}), & u<0 \end{cases} \tag{10}$$

where G is a proportionality constant describing the zero current conductivity. For sufficiently large $|u|$, only the exponential in nu will be important and $|J|$ will be given by

$$|J| \simeq Gce^{-\phi}e^{n|u|}. \tag{11}$$

This result can be compared with Eq. (7) which at large $|u|$ would reduce to Eq. (11) with $n=1/2$. We thus note an immediate consequence of a flattened barrier; since n is now less than 1/2, the exponential current does not rise as steeply with voltage as it does for a triangular barrier. This is not a small effect. For example, at 100 mV ($u=4$), with $n=0.3$, the current given by a flat barrier would be less by a factor of 2.2 than for a triangular barrier showing the same zero current conductivity. It is a significant observation that many lipid bilayers with carrier-mediated transport show currents less than would be predicted by a value of $n=1/2$, and exponential slopes (i.e., slopes of log I *vs.* V curves) of less than 1/2 at large voltage (*see*, for example, Szabo *et al.*, 1969)[3].

We can generalize now the results for the trapezoidal barrier to the case of asymmetric solutions with left-hand concentration c_1 and the right-hand concentration c_2 and note, by following the arguments which led to Eq. (10),

3 It should be noted that a $u/2$ exponential slope is built into any *single jump* Eyring model and that for a true exponential slope of less than $u/2$, at least two jumps must be used. (Jumps might, for example, be placed at positions corresponding to the corners of the trapezoidal barrier. Our approximations in this section reduce essentially to such treatment.)

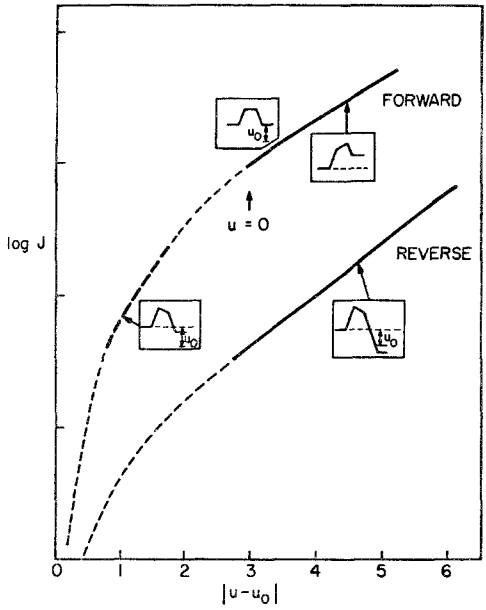

Fig. 4. Schematic current-voltage curves showing the barrier shape for different regions of voltage dependence. Voltage is plotted as a function of $u-u_0$ to show both directions of current on the same graph. In the "forward" curve, the voltage is negative and the current flow is from right to left. In the "reverse" curve, the voltage is positive and the current flow is from left to right

that

$$J=\begin{cases} Ge^{-\phi}(c_1 e^{nu}-c_2 e^{-(1-n)u}), & u>0 \\ Ge^{-\phi}(c_1 e^{(1-n)u}-c_2 e^{-nu}), & u<0. \end{cases} \tag{12}$$

At zero current, the barrier will now, by virtue of the asymmetry in concentration, have the form shown in Fig. 3*b*. If we apply a voltage so as to increase the height of the barrier for ions going right to left (ions from c_2, the high concentration side), the current will eventually vary as $c_1 e^{nu}$ because the second term will again have become negligible. The current at large voltages on either side of the resting potential will therefore be proportional to $e^{n|u|}$ as shown by the solid lines in Fig. 4, where we plot current in both directions on the same axis against $|u-u_0|$. The insets show the shape of the barrier for various current-voltage combinations. The curve labeled "forward" corresponds to the situation shown in Fig. 3*d* with $u<u_0$; the curve labeled "reverse" corresponds to the situation shown in Fig. 2*a* with $u>u_0$. Note that because of the convention chosen on the sign of the voltage, the "forward" direction corresponds to voltages less than u_0 and the "reverse" to voltages greater than u_0.

What happens in the intermediate case where the voltage is not very different from u_0? For the reverse curve in Fig. 4, clearly the current will

simply approach zero as u approaches u_0. This is shown by the dotted line. The case of the forward curve is more interesting. For situations like that shown in Fig. 3*c* where u lies between u_0 and zero, the left-hand corner of the trapezoid will still be important for current flow from right to left. If c_2 is sufficiently greater than c_1, the c_2 current will be dominant for a small voltage range as the barrier changes from the form of Fig. 3*b* to that of Fig. 2, and the current will have the voltage dependence given by

$$J \cong -Ge^{-\phi} c_2 e^{-(1-n)u}, \quad 0<u<u_0. \tag{13}$$

This is clearly a steeper curve than that for $|u| \gg u_0$, since $1-n$ is greater than n. This transition region is shown by the heavy dashed line in Fig. 4. It should be noted that near $u=0$ the barrier is flat and the I–V curve in this region will therefore be influenced by the shape of the top of the barrier.

We can also see that for this behavior there is substantial rectification about the resting potential for asymmetric concentrations ($c_1 \neq c_2$). We might also expect the dependence of zero current conductivity on the concentrations to be different. This is easily seen explicitly. We write the equation corresponding to Eq. (9) but for a trapezoid instead of a triangle barrier:

$$J=\begin{cases} Ge^{-\phi} c_1 e^{nu_0}(e^{n\Delta u}-e^{-(1-n)\Delta u}), & u \geqq 0 \\ Ge^{-\phi} c_1 e^{(1-n)u_0}(e^{(1-n)\Delta u}-e^{-n\Delta u}), & u \leqq 0. \end{cases} \tag{14}$$

For $|\Delta u|$ sufficiently large

$$J \cong \begin{cases} J(+\Delta u)=Ge^{-\phi} c_1 e^{nu_0} e^{n\Delta u}, & \Delta u \gg 0 \\ J(-\Delta u)=-Ge^{-\phi} c_1 e^{(1-n)u_0} e^{+n\Delta u}, & \Delta u \ll 0. \end{cases} \tag{15}$$

The rectification ratio is therefore given by

$$\frac{J(+\Delta u)}{J(-\Delta u)}=e^{(2n-1)u_0}=\left(\frac{c_2}{c_1}\right)^{2n-1}. \tag{16}$$

If $n=1/2$, the rectification ratio is unity as expected. To find the zero current conductivity we can expand the exponentials in Eq. (14) for small Δu and we see

$$J \cong Ge^{-\phi} c_1 e^{nu_0} \Delta u, \quad |\Delta u| \ll 1,$$

$$\frac{J}{\Delta u}=Ge^{-\phi}[c_1^{(1-n)} c_2^{n}] \tag{17}$$

which can be contrasted with the $\sqrt{c_1 c_2}$ dependence for the triangular barrier [Eq. (9)].

The point of the preceding discussion, then, was to show intuitively that the *barrier shape* influences three things: (a) the shape of the I–V curve;

(b) the dependence of zero current conductivity on the concentrations; and (c) dependence of the rectification ratio on the concentration. We consider these to be important but not generally recognized consequences of barrier shape. In particular, a barrier or hopping model which gives rise to a $\sinh(u/2)$ type of I–V curve for a particular region of experimental conditions *will not*, in that region, give rise to rectification about the resting potential.

Inversion of I–V Curves

It is clear that the two barrier shapes discussed in the previous section are not likely to be strictly exemplified by any real system. Physical barriers are likely to be more rounded although they should nevertheless show somewhat the same trends as the two cases we have discussed. Thus, a barrier with a flattened top should show more rectification than one with a fairly sharp peak, for example.

To deduce the barrier shape in bilayer membranes, we want to devise a method that will allow us to infer from the experimentally observed I–V curves the shape of the barrier underlying the I–V behavior. We begin by observing that all of the information about the barrier in Eq. (3) is contained in the integral in the denominator. We can therefore define a function $S(u)$ as

$$S(u)=\frac{c_1 e^{+u/2}-c_2 e^{-u/2}}{J(u)_{\text{exp}}} \tag{18}$$

(having the dimensions of $\text{cm}^{-1}\,\text{amp}^{-1}$ when the concentrations are in cm^{-3} and J is in amp/cm^2). By comparison with Eq. (3), $S(u)$ is given in terms of the barrier shape as

$$S(u)=\frac{1}{2eD}\int_{-1}^{1} e^{\left[\frac{u\xi}{2}+\omega(\xi)\right]}\,d\xi. \tag{19}$$

Clearly, a necessary condition that the model be applicable is that $S(u)$ *be only a function of voltage.* One can therefore measure I–V curves over a wide range of concentrations in symmetric and asymmetric solutions and determine whether the same function $S(u)$ describes all the I–V curves. If it does, it is worth pursuing the question further and solving the integral Eq. (19) for $\omega(\xi)$. We will now proceed to carry out this program for a particular experimental system.

Choice of Experimental System

To test Eq. (3), we must find an experimental system where the conditions of applicability of Eq. (3) are satisfied. That is, an energy barrier

must be the rate-limiting step to the movement of a single monovalent species across the membrane between two reservoirs of well-defined concentration. The reservoirs as well as the structure of the membrane must remain unaltered in the presence of an applied electric field. For such a system it is possible to infer unambiguously the shape of the energy barrier from the experimentally observed I–V relation.

Among the well-characterized experimental systems the extensively studied nonactin-induced potassium permeability of bilayers appears to best fulfill the above conditions. The identity of the charge carrier is known to be the potassium-nonactin complex, which forms with a 1:1 stoichiometry in the aqueous phases and presumably at the membrane surfaces as well (Szabo *et al.*, 1969; Läuger & Stark, 1970). Also, since the shape of the voltage-current curves of bilayers in the presence of nonactin and KCl remains unaltered when the KCl concentrations are varied over the range of 10^{-3} M to 1 M and for applied potentials at least as large as ± 200 mV (Hall, Mead & Szabo, *unpublished results*) one may conclude that the same rate-limiting process remains important throughout this range. Furthermore, the absence of a limiting current in the I–V relationships as well as the absence of deviations from a simple proportionality between membrane conductance and KCl concentration up to at least 1 M KCl indicate that carrier gradients within the membrane are not limiting the rate of potassium transfer in that concentration range (Läuger & Stark, 1970; Stark & Benz, 1971; Ciani, Eisenman, Laprade & Szabo, 1972).

The requirement that the membrane interior be the rate-limiting step in the transfer of the permeant species (i.e., the nonactin-K^+ complex) and the condition of field independent concentrations in the reservoirs of permeant species will both be met if the reaction

$$K^+ + S^* \rightleftharpoons K^+ S^* \tag{20}$$

between the K^+ ion and the membrane-bound nonactin S* producing the permeant K^+-nonactin complex $K^+ S^*$ is near equilibrium.

Since data presently available for the K^+-nonactin system do not allow us to deduce unambiguously whether or not reaction (20) is at equilibrium, the validity of this condition must be regarded for the present as an *a priori* assumption. The validity of this assumption will be examined more closely in the Discussion.

Assuming now that Eq. (20) does not deviate significantly from equilibrium, we can evaluate the concentration of the charged complexes, $c^*_{K^+s^*}$, at the membrane surface:

$$c^*_{K^+s^*} = K_s c^+_K c^*_s. \tag{21}$$

We can relate the concentration of nonactin c_s^* in the membrane to its known value c_s in the aqueous phase by a partition coefficient k_s

$$c_s^* = k_s c_s. \tag{22}$$

The concentration of charge-carrying complex at the surface will then be given by

$$c_{K^+ s}^* = K_s k_s c_s c_{K^+}. \tag{23}$$

It is clear that our original formulation for the current flow as a function of voltage applies to the movement of K^+-nonactin complexes across a barrier. We can thus replace c_1 and c_2 in our previous treatment by the appropriate concentration of the complex on each side of the membrane and the current will be given by

$$J = \frac{2eD}{d} \frac{k_s K_s c_s (c_{K_1^+} e^{u/2} - c_{K_2^+} e^{-u/2})}{\int_{-1}^{1} e^{\left(\frac{u\xi}{2} + \omega(\xi)\right)} d\xi}. \tag{24}$$

We have implicitly assumed the same concentration of nonactin on both sides for simplicity. It will be shown that Eq. (24) is valid over nearly the entire range of experimental conditions.

Materials and Methods

Membranes were formed from a 15-mg/ml solution of readily available bacterial phosphatidyl ethanolamine (Supelco 04-6040) in decane. Membrane-forming solution was sucked up in a pipette and squirted at a small hole in the septum of a Teflon chamber with two compartments of about 25-ml capacity. This technique allowed using a minimum amount of membrane solution and together with the use of chlorided silver electrodes, minimized the accidental introduction of contaminants (Szabo *et al.*, 1969). Nonactin was a gift from Miss Barbara Stearns of Squibb. It was dissolved in ethanol at a concentration of 10^{-3} M. Small aliquots of this stock solution were added to both sides of the membrane to obtain the desired antibiotic concentration in the aqueous phase. Equal volumes of ethanol without antibiotic had no effect on membrane conductance. Reagent grade potassium chloride was prepared as a stock solution and small aliquots added to increase the concentration. In the case of asymmetric solutions, aliquots of equal volume but different concentration were added to both sides to minimize pressure differentials which might disturb the membrane. To avoid ionic strength effects (Szabo *et al.*, 1969) such as might arise from charge on the surface of the membrane (McLaughlin, Szabo, Eisenman & Ciani, 1970), relatively impermeant LiCl was used to maintain a minimum ionic strength of 0.1 M.

The electrical apparatus used consists of a differential electrometer, a current-measuring operational amplifier and a voltage generator which can sweep the voltage at rates from 0.003 mV/sec to 4000 mV/sec. In these experiments, the rate of sweep never exceeded 12 mV/sec and was generally less than about 4 mV/sec. In any case, controls were done to insure that the rate of sweep was sufficiently slow so as not to

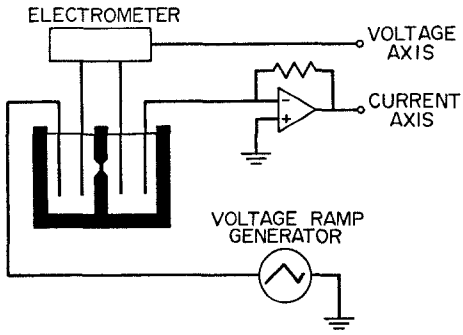

Fig. 5. Schematic diagram of the experimental apparatus. An X–Y plotter was used to record the current-voltage curves directly

affect the results. Silver-silver-chloride electrodes were used in a four-electrode system, and the I–V curves were traced directly on an X–Y recorder. A schematic drawing of the apparatus is shown in Fig. 5. The solutions on both sides were stirred with Teflon-coated magnetic fleas during measurements. The following experimental procedure was used to insure that no inaccuracies resulted from possible loss of antibiotic during the course of an experiment. Since the zero current conductivity of symmetric solutions with constant antibiotic concentration depends linearly on the aqueous concentration of carried ions (in the present case, potassium), each measurement of an I–V curve with asymmetric solutions was surrounded temporally by two I–V curves with symmetric solutions. For example, a given run might proceed in the following manner: a measurement might be taken with 10^{-3} M KCl solutions on both sides. A small aliquot of concentrated (4 M) KCl would then be added to the front chamber of the measuring cell to give solutions of 10^{-3} M and 10^{-2} M. After measuring the I–V curve, an identical aliquot would be added to the back to give solutions of 10^{-2} M on both sides and so on up to the maximum concentration of 1 M on both sides. If the zero current conductivities of the *symmetric* solutions failed to be linear in concentration, the data were not used. In this way, data reproducible on an absolute level to better than *10%* were obtained. The membrane area was measured visually at a magnification of 50 × with a calibrated reticule.

Results

Data from I–V curves in both symmetric and asymmetric solutions were used to calculate the function $S(u)$ as defined in Eq. (18), but with c_1 and c_2 denoting the KCl concentrations at the left- and right-hand sides of the membrane. The experimental values of $S(u)$ are plotted in the practical units, (moles/cm^3) per (amp/cm^2), in Fig. 6. All of these points were then fitted to a least-squares polynomial. Only even powers of u were used since $S(u)$ can be seen to be an even function of u by inspection of Eq. (19). This polynomial is the continuous curve plotted in Fig. 6. Since this polynomial gives a good fit, it is clear that $S(u)$ is *not* a function of concentration within the limits of experimental error. Consequently, the prerequisite for the model to be useful has been satisfied experimentally for the nonactin system

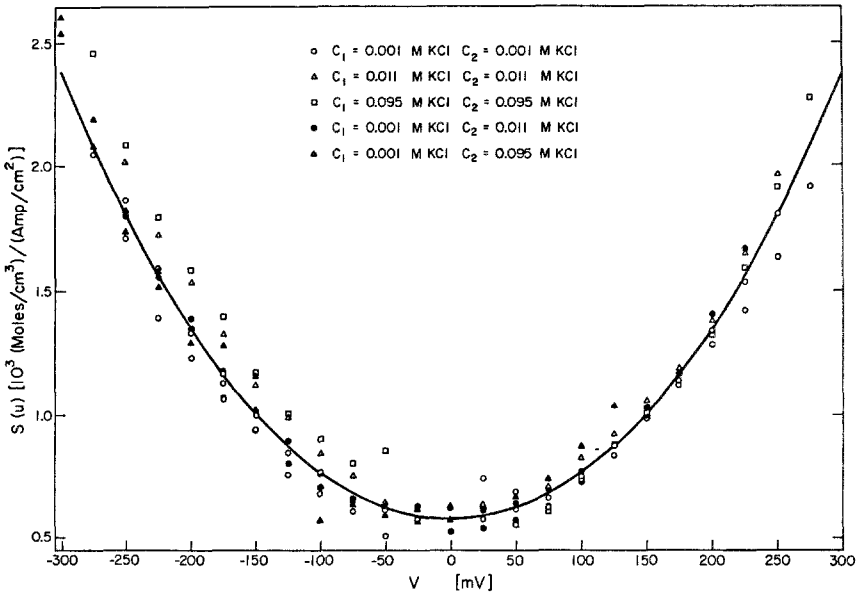

Fig. 6. The function $S(u)$ as calculated from Eq. (18) taking c_1 and c_2 as the aqueous KCl concentration. Symmetric concentrations are shown by open symbols and asymmetric concentrations by closed symbols. This function contains all information on the shape of the barrier and is seen to be a function of voltage only within an experimental error

and we can proceed with confidence to analyze $S(u)$ to deduce a shape for the barrier. It should be noted that the units in which $S(u)$ is measured have no effect on the voltage dependence of $S(u)$ or on the shape of the polynomial fit. A different choice of units would have resulted in polynomial coefficients differing only by a constant factor, and would correspond to the fact that the units of $S(u)$ are determined by the units of the diffusion constant, and those of the membrane thickness, the electric charge and the concentration in Eqs. (20) and (25). (In Eq. (25), $k_s K_s C_s$ is dimensionless.)

Interpretation as a Particular Barrier Shape

From Fig. 6 we know that a single experimentally measured form of the integral function $S(u)$ fits the data over a wide range of concentrations. It is therefore worthwhile to see if a physically reasonable barrier can explain the observed form of the integral and consequently the observed I–V curves. We therefore proceed to solve the integral equation

$$\int_{-1}^{1} e^{\left[\frac{u\xi}{2}+\omega(\xi)\right]} d\xi = \frac{2eD k_s K_s c_s}{d} S(u) \tag{25}$$

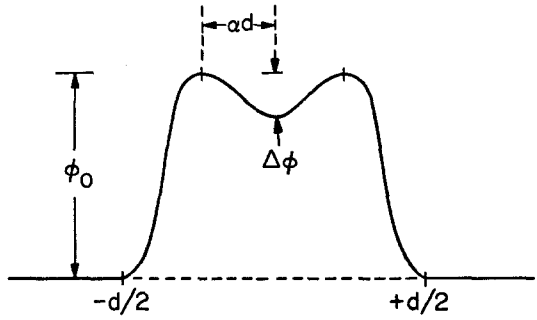

Fig. 7. The physical meaning of the parameters in Eq. (28). ϕ_0 is the height of the inflection point, α measures the position of the inflection point and corresponds roughly to $(1-n)/2$ for the trapezoidal barrier of Fig. 2. $\Delta\phi$, which can be either positive or negative, allows either a peak or a dip at the center of the membrane. This form was found to give the most satisfactory solution to the integral equation [Eq. (27)] for $S(u)$

for $\omega(\xi)$. All of the constants have their previously assigned meanings and $S(u)$ is calculated from experimental data according to Eq. (18). Note that because of the experimental units of $S(u)$, e in this equation is the charge of one mole (i.e., 1 Faraday). We can formally write

$$e^{\omega_0} = \frac{2eD}{d} k_s K_s c_s \tag{26}$$

where e^{ω_0} is a constant that will depend on the units in which the various parameters are measured. Note that this will determine the units of $S(u)$. Eq. (25) may then be rewritten in the form

$$S(u) = \int_{-1}^{1} e^{\left(\frac{u\xi}{2} + [\omega(\xi) - \omega_0]\right)} d\xi. \tag{27}$$

Thus, even though we do not know most of the parameters on the right-hand side of Eq. (26), we can nonetheless examine the *shape* of the barrier to within a constant additive factor by inversion of Eq. (27) for $\omega(\xi) - \omega_0$. We now choose as a sufficiently general function

$$\omega(\xi) = \begin{cases} \phi_0 - \dfrac{\Delta\phi}{2}\left(1 + \cos\dfrac{\pi\xi}{\alpha}\right), & |\xi| < \alpha \\ \dfrac{\phi_0}{2}\left\{1 + \cos\pi\left(\dfrac{|\xi| - \alpha}{1-\alpha}\right)\right\}, & |\xi| > \alpha. \end{cases} \tag{28}$$

This function gives a smooth barrier with continuous derivatives and allows, through $\Delta\phi$, either a peak or a dip in the center. Fig. 7 shows the geometric meanings of these parameters.

If we now measure $S(u)$ in units of $(\text{moles/cm}^3)/(\text{amps/cm}^2)$ and set the magnitude of $e^{-\omega_0}$ at 10^{-3}, we can use Eq. (28) to give the best fit to the

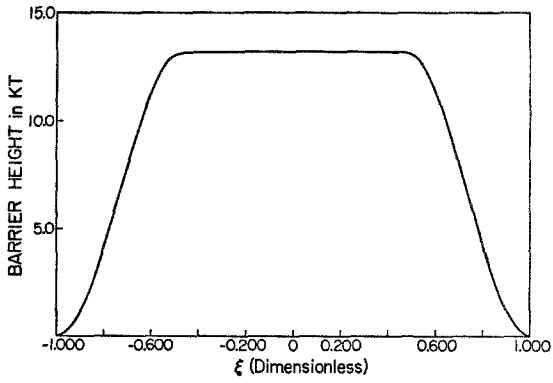

Fig. 8. The barrier shape as determined by the solution of Eq. (27). The height of the barrier is *not* measured accurately, but the flat top and position of the corners are sensitive to the experiment and are accurately determined. The values of the parameters are: $\phi_0 = 13.2$ kT, $\Delta\phi = 0.02$ kT, $\alpha = 0.47$. (An $\alpha = 0.47$ corresponds roughly to a value of $n = 0.27$ in Fig. 2)

values of $S(u)$ over the experimental range of roughly ± 300 mV. We find that ϕ_0 is then about 13 kT and that the barrier has the shape shown in Fig. 8. We know that a reasonable estimate of the energy difference of a complex at the edge of the membrane from one in the interior can be obtained by using the Born expression (Neumcke & Läuger, 1969*b*)

$$\phi = \frac{e^2}{r_{\text{ion}}}\left(\frac{1}{\varepsilon_{\text{mem}}} - \frac{1}{\varepsilon_{\text{aq}}}\right).$$

If we use $\varepsilon_{\text{mem}} \sim 2.0$, $\varepsilon_{\text{aq}} \sim 80$ and take r_{ion} to be the radius of the K^+-nonactin complex (about 10 Å), we calculate a value of energy difference of about 14 kT. Since 13 kT is quite close to the value we calculate from the Born expression, we conclude that $e^{-\omega_0}$ has a value within a few orders of magnitude of 10^{-3} as measured in (coul cm)/(mole sec). Our measurement is clearly not sensitive to the value of $e^{-\omega_0}$. This can be seen by observing that the contribution of the center of the barrier is going to be about 10^4 (e^{10}) greater than that of the edges as long as ϕ_0 is greater than about 10 kT. Thus, if we were to choose values of $e^{-\omega_0}$ in the range 10^{-1} to 10^{-5}, ϕ_0 would change by ± 4 kT, but the parameters α and $\Delta\phi$ would not change significantly and *these are the factors determining the voltage dependence.* The other parameters ϕ_0, D, k_s, and K_s are all lumped together in determining the zero current conductivity and are not significant in determining the form of the voltage dependence. As a direct check on this procedure the barrier of Fig. 8 was used to calculate the I–V curves from Eq. (24).

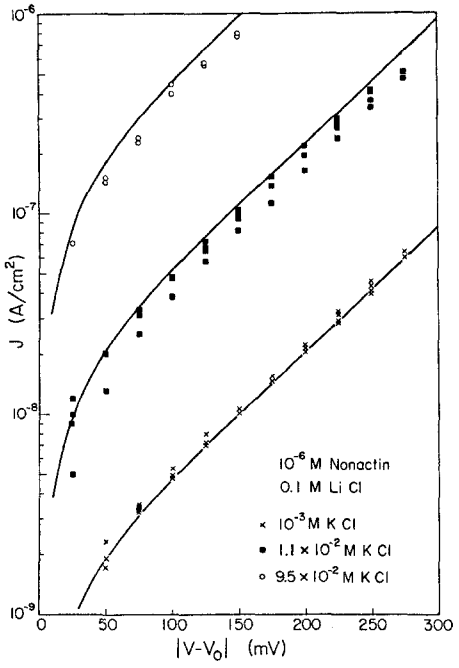

Fig. 9. Voltage-current curves for symmetric KCl concentrations. Positive and negative current directions are plotted on the same curve. The solid curves are calculated from the polynomial form of $S(u)$ shown in Fig. 6. Note that the fit is excellent at low concentrations and low voltages, but that at high voltage and high concentrations, the measured current is less than predicted presumably because under these conditions surface rate limiting is not totally negligible

Fig. 9 shows the experimental I–V curves in the case of symmetric potassium concentrations for three concentrations. The solid line is calculated using Eq. (24) and the barrier of Fig. 8. Note that the fit is excellent. In particular, the exponential dependence at higher voltages (which results in a straight line on the semilog plot of Fig. 9) is accurately predicted by the barrier shape. Fig. 10 shows the experimental I–V curves resulting from asymmetric potassium concentrations. The symmetric curve for 10^{-3} M potassium is shown for reference. "Forward" and "reverse" directions are plotted simultaneously to show the very evident rectification. Open symbols indicate the "reverse" direction and closed symbols the "forward" direction. Again the agreement is excellent. In particular, note that the rectification manifested by the separation of the curves and the exponential slopes at large voltages are well described by the barrier function of Fig. 8. In fact, the fit is *better* than that derived from the polynomial form of $S(u)$ and shows quite clearly that the model is capable of accounting for all of the

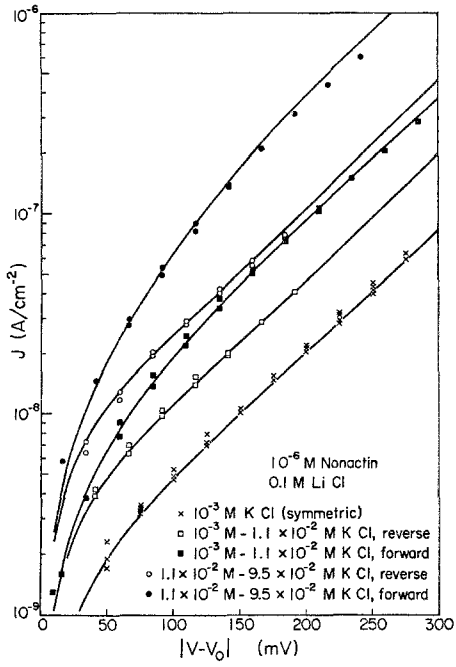

Fig. 10. I–V curves for asymmetric KCl concentrations. The lowest curve is the 10^{-3} M symmetric curve of Fig. 9 repeated for comparison and includes positive and negative currents. For the other curves, open symbols indicate positive (left-to-right) currents and closed symbols indicate negative (right-to-left) currents. Note the increase in the rectification, indicated by increased separation of the closed and open symbol curves, as the asymmetry of the concentrations is increased

data. We proceed to examine the results in more detail in the context of the earlier intuitive discussion.

Since the barrier is nearly trapezoidal we should expect the rectification ratio and the zero current conductivity to be similar to those derived in the intuitive discussion section for a trapezoidal barrier. The experimental barrier is very nearly the same as the barrier in Fig. 2 with $n=0.28$. According to Eq. (17), the rectification ratio should therefore be approximately given by (c_2/c_1) -0.44 for large Δu. This approximation is plotted as the dashed line in Fig. 11. The experimental points are calculated from the data of Fig. 10. It is clear that there is more rectification as the concentrations become more asymmetric. It is also readily apparent that the basic form of the rectification dependence is as expected from a roughly trapezoidal barrier. Indeed, if the calculation of rectification ratio from the barrier is performed without approximation, the solid line of Fig. 11 is obtained. This is a very good fit.

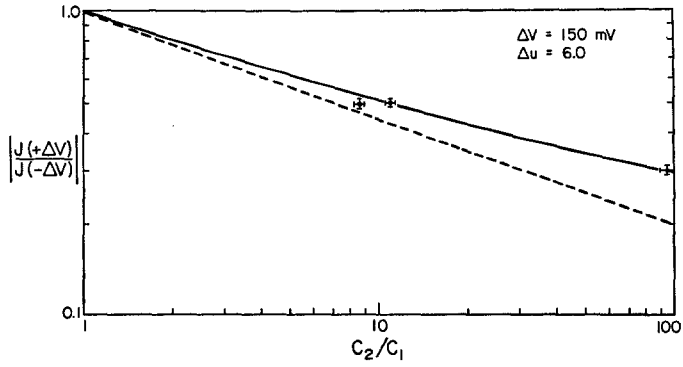

Fig. 11. Rectification at 150 mV as a function of concentration ratio, plotted on logarithmic scales. The solid line shows rectification as calculated from the model with the barrier function of Fig. 8. The dashed line shows the rectification, calculated using Eq. (16) with $n=0.28$ for the rectangular barrier approximation

The zero current conductivities in asymmetrical salt solutions are also as expected for a trapezoidal barrier with appropriate n value of 0.28 but the accuracy of measurement is not sufficiently good to draw conclusions on the basis of zero current conductivity data alone.

The model thus satisfactorily explains the experimental results, even out to several hundred millivolts, with only small deviations. We emphasize that the consequences of barrier shape, (a) shape of I–V curve, (b) dependence of rectification on concentration ratio, and (c) zero current conductivity dependence on concentrations, have all been successfully demonstrated to be within the framework of the model. The *a priori* assumption that the voltage dependence of the important rate-limiting step is sinh $(u/2)$ or the use of a *single-jump* Eyring treatment have been shown to be insufficiently accurate to describe the experimental results in the case of the nonactin-K^+ system.

Discussion

There are several objections which might be raised at this point. First, the membrane thickness and area can change with voltage. Capacitive measurements support the view that thickness decreases with increasing voltage (White, 1970). $S(u)$, on the other hand, *increases* with voltage experimentally. In any case, the percentage change in $S(u)$ is much too large to be accounted for by thickness change even if it were in the correct direction. Area change is a slightly greater problem. Area may increase slightly with

applied voltage. This means that $J(u)_{exp}$ is increasingly larger than it should be as the voltage increases and that $S(u)$ is increasingly *smaller* than it should be. This would not change the basic conclusions and here again the percentage change must be small, certainly less than 10% by capacitance measurements[4], and is not nearly sufficient, therefore, to explain the observed results.

There are, however, more serious objections to our interpretation of the experimental data. The most important of these is the question of whether or not the surface reaction [Eq. (20)] is really at equilibrium.

By careful consideration of our experimental data, we can show that deviations from equilibrium of reaction (20) (i.e. surface rate limiting) cannot easily account for the shape of the observed I–V relations at least where a sharp energy barrier in the center of the membrane is assumed[5]. Such a model has been proposed by Läuger and Stark (1970) and verified experimentally using the carrier valinomycin for which the surface reaction corresponding to Eq. (20) can be driven out of equilibrium (Stark & Benz, 1971). For the above model, Läuger and Stark derived the following expression for the current density J in symmetrical salt solutions:

$$J = R \frac{\sinh(u/2)}{1 + A\cosh(u/2)} \tag{29}$$

where R is a proportionality constant dependent on carrier, salt concentration and membrane composition. The voltage independent parameter A measures the extent to which reaction (20) is displaced from equilibrium[6]. For the nonactin-K^+ system, both the strict proportionality of zero current membrane conductance to the KCl concentration and the independence of the shape of I–V curves on concentration up to 1 M KCl in symmetrical salt solutions imply that A is independent of the KCl concentration. Consideration of our experimental data indicates that Eq. (29) cannot adequately

4 Voltage dependence of capacitance was measured in our laboratory with films of composition identical to those which were used in this study. The results essentially agree with those of White, 1970.

5 Preliminary results of relaxation experiments similar to those of Stark *et al.* (1971) but performed using nonactin and trinactin, indicate that reaction (20) is likely to be near equilibrium for the lipid and the range of concentrations examined in this paper (Laprade, Ciani, Eisenman & Szabo, *personal communication*).

6 Note that more generally the parameter A also accounts for such nonequilibrium effects as carrier gradients in the membrane interior as well as rates of transfer of complexes from the aqueous phase across the membrane surfaces (*see* Stark & Benz, 1971). For the nonactin-K^+ system, the strict proportionality of the zero current concentration implies that carrier gradients are negligible.

predict the I–V relationship for the nonactin-K^+ system unless the parameter A is allowed to vary as a function of the voltage[7].

We thus conclude that one must require A to be voltage dependent or use a different model to explain satisfactorily the experimental result.

In contrast, the same physically reasonable barrier shape can explain easily not only the result given above, but also I–V curves taken over a wide range of symmetric and asymmetric concentrations.

The second difficulty in our interpretation of the I–V results is the possibility that the barrier height may be a function of voltage. In fact it is not possible solely on the basis of I–V curve measurements to distinguish formally between a sharp barrier which is a function of coordinate and a barrier which is some special function of voltage. In other words, the integral equation for $S(u)$ [Eq. (20)] can be solved only if ω is a function either of ξ only or of u only. There are, however, some inductive arguments which show that a barrier whose height is primarily a function of position is more physically reasonable than one whose height varies with voltage. It is not too unreasonable to assume that the change in barrier height with voltage can be approximated by the first power of u in a series expansion

$$\phi = \phi_0 + ku^2. \tag{30}$$

In this case, the current would be given by

$$J = \frac{eD\phi}{d} e^{-\phi_0 - ku^2}(c_1 e^{u/2} - c_2 e^{-u/2}). \tag{31}$$

It is then simple to show that the rectification ratio at large Δu would be

$$\left|\frac{J(+\Delta u)}{J(-\Delta u)}\right| = e^{-(4k\Delta u u_0)} = \left(\frac{c_2}{c_1}\right)^{-4k\Delta u}. \tag{32}$$

If $k=0$, the rectification ratio is 1, as required. For other values of k, this dependence is clearly different from the concentration dependence of the rectification ratios expected for the trapezoidal barrier, and therefore provides, in principle, a means of distinguishing between the two cases.

It is only possible to get the same dependence one gets with a trapezoidal barrier if one assumes that the barrier is given by

$$\phi = \phi_0 + k|u| \tag{33}$$

7 As a specific example, we find that the voltage current relation for 0.001 M salt can be best fit by an A value of 0.02. At first glance, the fit appears reasonable; but on closer inspection, it becomes apparent that the slopes of data and the theory disagree markedly. In the case of the data, the logarithmic derivative saturates at about 100 mV with a value of 0.35 but Eq. (26) predicts a value of 0.40 which then decreases steadily to a value of 0.17 at 250 mV, where the experimental slope is still 0.35.

and is quite sharp. But we also know that a sharp barrier is inconsistent with the image force shape expected from the calculation of Neumcke and Läuger (1969*b*).

It is also quite likely that the image force is an important contribution to the shape of the barrier. Indeed, the barrier of the shape of Fig. 10 is very close to that expected from the image force calculation of Neumcke and Läuger (1969*b*). Thus, since the barrier we measure is close to that expected for the distance dependent image force, we can feel safe in concluding that the barrier height is indeed a function of position and not of voltage.

We conclude therefore that the Nernst-Planck treatment with a barrier of the shape shown in Fig. 8 is adequate to explain the I–V curves of the nonactin-K^+ system and that the assumption of a single jump Eyring treatment of sinh ($u/2$) barrier is inadequate. Although this model may not be unique in predicting the observed results, it has the virtues of simplicity and physical plausibility.

We wish to thank Dr. Stuart McLaughlin and Professors Max Delbrück and George Eisenman for critical readings of the manuscript.

J. E. H. thanks the Sloan Foundation for support. G. S. acknowledges the support of USPHS Grant No. NS 09931-02 and NSF Grant No. GB 30835.

References

Andreoli, T. E., Tieffenberg, M., Tosteson, D. C. 1967. The effect of valinomycin on the ionic permeability of thin lipid membranes. *J. Gen. Physiol.* **50**:2527.

Buzhinsky, E. P. 1968. Current-voltage dependences of the bimolecular phospholipid membranes with incorporated valinomycin. *Citologia* (*U.R.S.S.*) **10**:1432.

Ciani, S., Eisenman, G., Laprade, R., Szabo, G. 1972. Theoretical analysis of carrier-mediated electrical properties of lipid bilayers. *In:* Membranes – A Series of Advances, Vol. 2. G. Eisenman, editor. Marcel Dekker, New York. (*In press.*)

Hanai, T., Haydon, D. A., Taylor, J. 1965. The variation of capacitance and conductance of bimolecular lipid membranes with area. *J. Theoret. Biol.* **9**:433.

Laprade, R., Ciani, S. M., Szabo, G., Eisenman, G. 1972. Equilibrium and kinetic "domains" for trinactin effects on bilayer membranes. *Biophys. Soc. Abstr.* **12**:44a.

Läuger, P., Stark, G. 1970. Kinetics of carrier-mediated ion transport across lipid bilayer membranes. *Biochim. Biophys. Acta* **211**:458.

Lev, A. A., Buzhinsky, E. P. 1967. Cation specificity of the model bimolecular phospholipid membranes with incorporated valinomycin. *Citologia* (*U.R.S.S.*) **9**:102.

McLaughlin, S. G. A., Szabo, G., Eisenman, G., Ciani, S. 1970. Surface charge and the conductance of phospholipid membranes. *Proc. Nat. Acad. Sci.* **67**:1268.

Mueller, P., Rudin, D. O. 1967. Development of K^+-Na^+ discrimination in experimental bimolecular lipid membranes by macrocyclic antibiotics. *Biochem. Biophys. Res. Commun.* **26**:398.

Mueller, P., Rudin, D. O., Tien, H. Ti, Wescott, W. C. 1962. Reconstitution of excitable cell membrane structure in vitro. *Circulation* **26**:1167.

Neumcke, B., Läuger, P. 1969*a*. Space charge-limited conductance in lipid bilayer membranes. *J. Membrane Biol.* **3**:54.

Neumcke, B., Läuger, P. 1969*b*. Non-linear electrical effects in lipid bilayer membranes. II. Integration of the generalized Nernst-Planck equation. *Biophys. J.* **9**:1160.

Pioda, L. A. R., Wachter, H. A., Dohner, R. E., Simon, W. 1967. Komplexe von Nonactin und Monactin mit Natrium-, Kalium- und Ammonium-Ionen. *Helv. Chim. Acta* **50**:1373.

Pressman, B. C. 1968. Ionophorous antibiotics as models for biological transport. *Fed. Proc.* **27**:1283.

Shemyakin, M. M., Ovchinnikov, Yu. A., Ivanov, V. T., Antonov, V. K., Vinogradova, E. I., Shkrob, A. M., Malenkov, G. G., Evstratov, A. V., Laine, I. A., Melnik, E. I., Ryabova, I. D. 1969. Cyclodepsipeptides as chemical tools for studying transport through membranes. *J. Membrane Biol.* **1**:402.

Stark, G., Benz, R. 1971. The transport of potassium through lipid bilayer membranes by the neutral carriers valinomycin and monactin. Experimental studies to a previously proposed model. *J. Membrane Biol.* **5**:133.

Stark, G., Ketterer, B., Benz, R., Läuger, P. 1971. The rate constants of valinomycin mediated ion transport through thin lipid membranes. *Biophys. J.* **11**:81.

Szabo, G., Eisenman, G., Ciani, S. 1969. The effects of the macrotetralide actin antibiotics on the electrical properties of phospholipid bilayer membranes. *J. Membrane Biol.* **1**:346.

Tosteson, D. C. 1968. Effect of macrocyclic compounds on the ionic permeability of artificial and natural membranes. *Fed. Proc.* **27**:1269.

Walz, D., Bamberg, E., Läuger, P. 1969. Non-linear electrical effects in lipid bilayer membranes. I. Ion injection. *Biophys. J.* **9**:1150.

White, S. H. 1970. Thickness changes in lipid bilayer membranes. *Biochim. Biophys. Acta* **196**:354.